PHYSICAL REVIEW D VOLUME 47, NUMBER 12 15 JUNE 1993

# Dynamics of the electroweak phase transition

Margaret E. Carrington
*Theoretical Physics Institute, University of Minnesota, Minneapolis, Minnesota 55455*
*and Physics Department, University of Winnipeg, Winnipeg, Manitoba, Canada R3B 2E9**

Joseph I. Kapusta
*School of Physics and Astronomy, University of Minnesota, Minneapolis, Minnesota 55455*
(Received 18 December 1992; revised manuscript received 19 March 1993)

We apply recent advances in equilibrium and nonequilibrium finite-temperature field theory to the dynamics of the electroweak phase transition in the early Universe. The equation of state and the parameters that enter the nucleation rate, including the preexponential factor, are calculated in the one-loop plus ring-diagram approximation in the standard model. The velocity of bubble growth is taken from a recent relativistic kinetic theory calculation. We compute the temperature, average bubble size, bubble density, and fraction of space which has been converted from the high-temperature symmetric phase to the low-temperature asymmetric phase as functions of time. Compared to the idealized adiabatic Maxwell construction of phase equilibrium, the start of the phase transition is significantly delayed, but then completes in a much shorter time interval.

PACS number(s): 98.80.Cq, 12.15.Ji, 64.60.Qb

## I. INTRODUCTION

It was predicted nearly twenty years ago that what is now known as the standard model of the electroweak interactions should undergo a phase transition at a temperature of order 100 GeV [1]. Below this temperature the $SU(2)\times U(1)$ gauge symmetry is spontaneously broken, above it the symmetry is restored. Such high temperatures are only imaginable in the early Universe. There has been a flurry of activity in this area of electroweak physics recently because of the possiblity that the present baryon number of the Universe was generated by baryon number changing processes [2] during the electroweak phase transition [3]. The nature of the electroweak phase transition and the dynamics of the expanding Universe during the phase transition demand our close attention.

In this paper, it is our intention to provide a detailed analysis of the dynamics of the electroweak phase transition in the early Universe. We shall assume the validity of the standard model without extra Higgs fields, although they may be necessary to generate the observed amount of baryon number [4]. The following are the essential ingredients for the study. First, knowledge of the equation of state of electroweak matter is required to solve Einstein's equations and to determine the parameters in the nucleation rate. We take the equation of state from the recent analysis of Carrington [5] who has summed the ring diagrams in addition to the usual one-loop contributions. The phase transition is weakly first order; this is fortunate because baryogenesis requires a first-order transition. The second necessary ingredient is the nucleation rate. It is composed of two parts: the exponential factor and the preexponential factor. The origin and form of the exponential factor are well known [6–9]; it is the exponential of minus the free energy of a critical-size bubble of the asymmetric phase floating in the symmetric phase. We determine this free energy on the basis of the effective potential as computed by Carrington [5] including finite bubble size effects [8–10]. An expression for the preexponential factor in terms of physical quantites, such as surface free energy, correlation length, latent heat, and viscosity was recently obtained by Csernai and Kapusta [11]. Again, these parameters are inferred from the effective potential of Carrington, except for the viscosity, which is computed in this paper. Finally, we need a rate equation for the time evolution of the phase transition. We use the rate equation as given by Csernai and Kapusta [12] which they applied to the QCD phase transition in high energy nuclear collisions. A necessary ingredient in this equation is the radial velocity of bubble growth; we take this from a recent analysis of Liu, McLerran, and Turok [10].

With this input we solve for the time evolution of the Universe as it passes through the electroweak phase mixture. In particular we compute, as functions of time, the temperature, the fraction of space which has been converted from the symmetric phase to the asymmetric phase, the average bubble size, and the average bubble separation. The time dependence of these quantities has been discussed before [13]. In this paper we calculate these quantities to the best accuracy available given our present understanding of equilibrium and nonequilibrium finite-temperature field theory.

This paper is organized as follows. In Sec. II we review the dynamics of nucleation and the rate equation which incorporates nucleation and growth of bubbles. In Sec. III we extract the electroweak equation of state,

*Present address.

 

the surface free energy, and the correlation length, all of which are needed for the nucleation rate. We analyze critical bubbles whose radius is not very much larger than the correlation length. In Sec. IV we obtain the radial growth velocity of bubbles from the recent analysis of Liu, McLerran, and Turok and express it in terms of our parameters. In Sec. V we compute the viscosity of electroweak matter in the high-temperature symmetric phase. Finally, we solve the coupled nonlinear integral and differential equations for the time evolution of the phase transition in the early Universe in Sec. VI. The results are interesting in their own right and should be useful for baryogenesis studies. We present conclusions and suggestions for further research in Sec. VII.

## II. REVIEW OF NUCLEATION THEORY

The rate for the nucleation of the low-temperature, asymmetric phase "$A$" out of the high-temperature, symmetric phase "$S$" can be written as [11, 14, 15]

$$I = I_0\, e^{-\Delta F_*/T}, \tag{1}$$

where $\Delta F_*$ is the change in the free energy of the system with the formation of a critical-size $A$-phase bubble and $I_0$ is the prefactor. In general, statistical fluctuations at $T < T_c$ will produce bubbles with radius $r$ with associated free energy

$$\Delta F = \frac{4\pi}{3}[p_S(T) - p_A(T)]r^3 + 4\pi r^2\sigma. \tag{2}$$

Here $p$ is the pressure of the $S$ or $A$ phase at temperature $T$, and $\sigma$ is the surface free energy of the $S$-$A$ interface. Since $p_S - p_A < 0$ it follows as usual that there is a bubble of critical radius

$$r_*(T) = \frac{2\sigma}{p_A(T) - p_S(T)}. \tag{3}$$

Smaller bubbles tend to shrink because the surface energy is too great relative to volume energy, and larger bubbles tend to grow. The free energy of the critical-size bubble is therefore

$$\Delta F_* = \frac{4}{3}\pi\sigma r_*^2. \tag{4}$$

This expression is valid if the radius of a critical bubble is large compared to the correlation length. We will discuss the free energy of small critical bubbles in the next section.

The prefactor has very recently been computed in a coarse-grained effective field theory approximation to be [11]

$$I_0 = \frac{16}{3\pi}\left(\frac{\sigma}{3T}\right)^{3/2}\frac{\sigma\eta_S r_*}{\xi_S^4(\Delta w)^2}, \tag{5}$$

where $\eta_S$ is the shear viscosity in the $S$ phase, $\xi_S$ is a correlation length in the $S$ phase, and $\Delta w$ is the difference in the enthalpy densities of the two phases. This prefactor is very similar to that calculated by Kawasaki [16] and by Turski and Langer [17] for nonrelativistic fluids near their critical points. The nucleation rate is limited by the ability of dissipative processes to carry latent heat away from the bubble's surface, as indicated by the dependence on the viscosity. At the critical temperature, $r_* \to \infty$, and the rate vanishes. The system must supercool at least a minute amount in order that the rate attain a finite value.

Given the nucleation rate one would like to know the (volume) fraction of space $f(t)$ which has been converted from the $S$ phase to the $A$ phase at the proper time $t$ as measured in the local comoving frame of an expanding system. This requires kinetic equations which use the nucleation rate $I$ as an input. Langer and Schwartz [18] have discussed such kinetic equations and compared predictions of their theory to cloud-point data in near-critical fluids. Guth and Weinberg [19] proposed a formula for $f(t)$ and applied it to cosmological first-order phase transitions. One may find other kinetic equations in the literature. It does not seem possible to derive such kinetic equations from first principles. Here we use a rate equation first proposed in [12]. The nucleation rate $I$ is the probability to form a bubble of critical size per unit time per unit volume. If the system cools to $T_c$ at time $t_c$ then at some later time $t$ the fraction of space which has been converted to the $A$ phase is

$$f(t) = \int_{t_c}^{t} dt' I(T(t'))[1 - f(t')]V(t', t). \tag{6}$$

$V(t', t)$ is the volume of a bubble at time $t$ which was nucleated at the earlier time $t'$; this takes into account bubble growth. The factor $1 - f(t')$ takes into account the fact that new bubbles can only be nucleated in the fraction of space not already occupied by the $A$ phase. This conservative approach does not take into account collisions and fusion of bubbles, which would tend to decrease somewhat the time needed to complete the transition [20].

Next we need a dynamical equation which couples the time evolution of the temperature to the fraction of space converted to hadronic gas. We use Einstein's equations as applied to the early Universe, neglecting curvature. The evolution of the energy density $e$ is

$$\frac{de}{dR} = -\frac{3w}{R}, \tag{7}$$

where $R$ is the scale factor at time $t$. This assumes kinetic but not phase equilibrium, and is basically a statement of energy conservation. We express the energy density as

$$e = f e_A(T) + [1 - f]e_S(T), \tag{8}$$

where $e_A$ and $e_S$ are the energy densities in the two phases at the temperature $T$. There is a similar equation for $w$. The time dependence of the scale factor is determined by the equation of motion

$$\frac{1}{R}\frac{dR}{dt} = \sqrt{\frac{8\pi G e}{3}}. \tag{9}$$

This expression can be used to rewrite the rate equation

in the alternate form

$$f(R) = \sqrt{\frac{3}{8\pi G}} \int_1^R \frac{dR'}{R'\sqrt{e(R')}} I(T(R')) \times [1 - f(R')] V(R', R). \quad (10)$$

We have chosen the normalization $R(t_c) = 1$. Because the Universe is expanding very slowly on the electroweak time scale ($t_c \approx 10^{-11}$ sec) and the phase transition is only weakly first order ($\Delta e \ll e$), it is a very good approximation to neglect the variation of $R'\sqrt{e(R')}$ in the denominator of the integrand of the rate equation above. Similarly, during the phase transition it is a very good approximation to integrate the equation of motion of $R$ to get

$$t - t_c = \sqrt{\frac{3}{8\pi G e(t_c)}} (R - 1) . \quad (11)$$

This is useful in relating the time into the transition to the amount of expansion of the Universe.

We also need to know how fast a bubble expands once it is created. This is a subtle issue since by definition a critical-size bubble is metastable and will not grow without a perturbation. We shall only attempt a crude description of this growth process here. After applying a perturbation, a critical-size bubble begins to grow. As the radius increases, the surface curvature decreases, and an asymptotic interfacial velocity is approached. The asymptotic radial growth velocity will be referred to as $v(T)$. The expected qualitative behavior of $v(T)$ is that the closer $T$ is to $T_c$ the slower the bubbles grow. At $T_c$ there is no motivation for bubbles to grow at all since one phase is as good as the other. Our simple illustrative model for bubble growth is

$$V(t', t) = \frac{4\pi}{3} \left( r_*(T(t')) + \int_{t'}^{t} dt'' v(T(t'')) \right)^3 . \quad (12)$$

This expression can also be written in terms of $R, R', R''$ instead of $t, t', t''$. As pointed out by Linde [6] one could argue for the insertion of the dilution factor $R(t')/R(t'')$ behind the integration symbol above. However, the Universe expands so terribly little during this very weak first-order transition that this is a negligible effect.

## III. EFFECTIVE POTENTIAL AND EQUATION OF STATE

One of us has computed the effective potential in the standard model by evaluating both the one-loop diagrams and the sum of ring diagrams [5]. The ring diagrams are necessary in this context because it turns out that the phase transition is very weakly first order and several of the scalar and vector boson masses are very small near the critical temperature. Infrared contributions to the effective potential become important as the boson masses go to zero, and it is well known that these contributions can be accurately taken into account by summing the ring diagrams [21, 22].

Let us denote the effective potential by $V_{\rm eff}(\phi, T)$ where $\phi$ is the value of the scalar condensate field. It turns out that with inclusion of the ring diagrams there is no simple analytic expression for this potential, it must be evaluated numerically. To a good approximation it looks very much like a fourth-order polynomial in $\phi$ with temperature-dependent coefficients. In the neighborhood of $T_c$ it has two minima, one corresponding to the $S$ phase at $\phi_S = 0$ and the other corresponding to the $A$ phase at $\phi_A > 0$. Above $T_c$ the global minimum is at the origin, below $T_c$ the global minimum is at $\phi_A$, and at $T_c$ the two minima are degenerate.

The thermodynamic pressure is the negative of the effective potential at the minimum. Thus

$$p_S(T) = -V_{\rm eff}(0, T)$$
$$p_A(T) = -V_{\rm eff}(\phi_A(T), T) . \quad (13)$$

The effective potential is normalized so that the pressure of the vacuum is zero. The pressure difference defined as $\Delta p = p_A - p_S$ is equal to zero at $T_c$ and is positive below $T_c$. We use a vacuum Higgs mass of 60 GeV and a top quark mass of 120 GeV, all other parameters are standard. With these parameters $T_c = 97.27$ GeV. For supercooling of up to 2% ($0.98T_c < T < T_c$) we have found an accurate parametrization of the pressure difference to be

$$\Delta p = (5.977x + 498.7x^2 - 7621x^3) \times 10^5 \ \text{TeV/fm}^3, \quad (14)$$

where $x = 1 - T/T_c$.

It is not necessary to know the absolute value of the pressure as accurately as the pressure difference. The pressure difference determines the size and free energy of critical-size bubbles as well as the bubble growth velocity. The magnitude of the pressure influences the expansion rate of the Universe, but since the Universe is expanding so slowly at this epoch, a few percent change in the absolute magnitude of the pressure has no real consequences for the phase transition. Close inspection of the expressions in [5] leads one to the approximate form of the pressure in the high-temperature phase as

$$p_S(T) = \frac{427}{360}\pi^2 T^4 - \frac{m_H^2}{8\sqrt{2}G_F}, \quad (15)$$

where $m_H$ is the zero-temperature Higgs mass and $G_F$ is the Fermi constant. The pressure in the low-temperature phase is $p_A = p_S + \Delta p$.

The entropy, energy, and enthalpy densities in each phase can be obtained via the canonical thermodynamic relationships

$$s = dp/dT,$$
$$e = -p + Ts, \quad (16)$$
$$w = e + p,$$

assuming that all chemical potentials are negligibly small. For the parameters chosen in this paper the ratio of the latent heat to the energy density in the $S$ phase at $T_c$ is very small:

$$\Delta e/e_S = \Delta w/e_S = (5.98 \times 10^5\,\mathrm{TeV\,fm^{-3}})/(4.13 \times 10^8\,\mathrm{TeV\,fm^{-3}}) = 1.45 \times 10^{-3} = 0.145\%.$$

This is a very weak first-order phase transition even though in a terrestrial sense the latent heat is huge.

The static correlation length $\xi$ for the scalar field is expressed in terms of the second derivative of the effective potential at a minimum:

$$\xi^{-2} = \frac{d^2 V_{\mathrm{eff}}}{d\phi^2}. \tag{17}$$

Static, spatial inhomogeneities in the scalar field fall off exponentially with this decay length, $\exp(-z/\xi)$. In general the correlation lengths in the two phases are different. For an effective potential that is quartic in the field they are the same at $T_c$. Even though the ring-improved effective potential is not exactly of the quartic form, we have found numerically that the curvatures at the minima are equal at $T_c$. The value is

$$\xi_A = \xi_S = 17.94/T_c = 0.0364\ \mathrm{fm}. \tag{18}$$

As the temperature decreases, the correlation length increases in the $S$ phase and decreases in the $A$ phase. Since we expect relatively little supercooling we shall neglect this temperature variation. This approximation could be relaxed if necessary.

The surface free energy at $T_c$ is given by the well-known expression [23]

$$\sigma = \int_{-\infty}^{\infty} dz \left(\frac{d\bar{\phi}}{dz}\right)^2, \tag{19}$$

where $\bar{\phi}(z)$ satisfies the classical equation of motion with the potential $V_{\mathrm{eff}}(\bar{\phi}, T)$. Since the potential is well-approximated by a fourth-order polynomial, we use the solution

$$\bar{\phi}(z) = \frac{\phi_A}{2}[1 + \tanh(z/2\xi)]. \tag{20}$$

The surface free energy then is

$$\sigma = \frac{\phi_A^2(T_c)}{6\xi}. \tag{21}$$

We find numerically that $\phi_A(T_c) = 0.5227\,T_c$. Therefore $\sigma = 60\ \mathrm{TeV/fm^2}$. It is problematical to rigorously define a surface free energy at any temperature other than $T_c$.

The free energy of critical-size bubbles is accurately described by Eq. (4) only when the radius is much greater than the correlation length, or equivalently stated, when the temperature approaches $T_c$. Deviations appear when $r_*$ becomes less than about ten times the correlation length. This is known both in molecular physics [24] and in field theory [6, 8–10]. This finite-size effect needs to be taken into account in rate calculations for the early Universe, because it has been estimated that the argument of the exponential in Eq. (1) is on the order of $-160$ when the transition occurs [7], and a 10% change in the free energy has a big effect when exponentiated.

In the following discussion we use the notation of [10]. The authors express the free energy in terms of a dimensionless integral

$$\Delta F/T \propto \int dr\, r^2 \left[\frac{1}{2}\left(\frac{dg}{dr}\right)^2 + \frac{\zeta}{2}g^2 - g^3 + \frac{1}{4}g^4\right], \tag{22}$$

where $g$ is a dimensionless field, $r$ is a dimensionless coordinate, and we shall not be concerned with the constant of proportionality. The parameter $\zeta$ is a function of the temperature. It has the value 2 at $T_c$ and decreases towards zero as the temperature decreases. The potential has local minima at $g_S = 0$ and at $g_A = (3+\sqrt{9-4\zeta})/2$. The profile $g(r)$ has been computed numerically for different values of $\zeta$ and the integral evaluated to yield the free energy; the results are presented graphically in Fig. 1 of [10]. The ratio $\Delta F(\text{finite size})/\Delta F(\text{volume+surface})$ can be read off of that figure. For $\zeta > 1.45$ an accurate (better than 1%) parametrization of this ratio is

$$\Delta F(\text{finite size}) = \Delta F(\text{volume} + \text{surface}) \times (g_A/2)^{4.5}. \tag{23}$$

Note that this correction factor extrapolates to unity at $\zeta = 2$.

The parameter $\zeta$ still needs to be related to other physical quantities to be useful in our rate equations. This can be done in one of two ways. One way is to take the scalar condensate $\phi$ as the independent field and to rescale it and the radial coordinate to put $\frac{1}{2}(\nabla\phi)^2 + V_{\mathrm{eff}}(\phi, T)$ in the dimensionless form used in [10], thereby extracting $\zeta$ (assuming the effective potential can be represented by a fourth-order polynomial). The other way is to take the local energy density $e$ as the independent field, as done in [11], and to rescale it and the radial coordinate to put the effective coarse-grained free energy functional in the dimensionless form. In [11] this free energy functional was parametrized as $\frac{1}{2}K(\nabla e)^2 + f(e)$, where $f(e)$ is a fourth-order polynomial and $K$ is a constant. The second way is actually the more convenient one. After some algebra, one can infer from the expressions given in [11] that

$$\zeta = \frac{18\chi}{(2+\chi)^2}, \qquad \chi = 1 + \frac{r_*}{4\xi} - \left[\left(\frac{r_*}{4\xi}\right)^2 + 1\right]^{1/2}, \tag{24}$$

where $r_*$ is given by the Young-Laplace equation (3). We shall apply this correction factor to the free energy [Eq. (4)] when computing the thermal nucleation rate. We shall not be concerned with any modifications to the preexponential factor due to finite-size effects.

## IV. BUBBLE GROWTH VELOCITY

The asymptotic growth velocity of bubbles was considered in detail by Liu, McLerran, and Turok [10]. They

used relativistic transport theory. Such a microscopic calculation is necessary in order to compute the velocity of the interface; energy and momentum conservation in perfect fluid dynamics is not sufficient.

We start from Eq. (111) of [10]. It is

$$\frac{9\pi}{4N_F}\frac{u}{T\ln(AT^2/M^2)}\int_{-\infty}^{\infty}dz\,\phi^2\left(\frac{d\phi}{dz}\right)^2=\Delta p\ . \tag{25}$$

Here $A$ is an as yet undetermined constant, $M$ is the vector meson mass in the $A$ phase, $N_F=48$ is the number of left-handed fermion degrees of freedom, $\Delta p$ is the pressure difference between the two phases, $\phi(z)$ gives the variation in the Higgs field across the interface, and $u=\gamma v=v/\sqrt{1-v^2}$ with $v$ the velocity. Since the constant $A$ is unknown we set the logarithm to one, as in [10].

For temperatures below but very close to $T_c$ the Higgs field follows the usual hyperbolic arctangent behavior as given in Eq. (20). The integration is simple, and gives

$$\frac{9\pi}{80N_F}\frac{\phi_A^4}{\xi T_c}u=\Delta p\ . \tag{26}$$

With the numerical values for $\phi_A, T_c, \xi$ as given in the previous section we get

$$u=3.26\times10^4\,\frac{\Delta p}{T_c^4}\ . \tag{27}$$

Thus the growth velocity vanishes as the temperature approaches $T_c$, as it should.

## V. VISCOSITY OF THE HIGH-TEMPERATURE PHASE

In this section we intend to compute the shear viscosity in the high-temperature $S$ phase in the relaxation time approximation. We shall only compute it to leading-log order in the coupling constants. This is sufficient for our purposes, since a factor of 2 error in the shear viscosity introduces a factor of 2 error in the exponential prefactor in the nucleation rate, and this will have a negligible influence on the numerical results which are dominated by the exponential factor. In the $S$ phase all particles are massless to zeroth order. The bulk viscosity is very small for a system of point particles with no internal rotational degrees of freedom. The shear viscosity must, on dimensional grounds, be of the form $cT^3$, where $c$ is a number. The whole thrust of this section is to compute $c$. The reader who only wants to know the answer can turn to the last line of this section.

The shear viscosity ($\eta$) and bulk viscosity ($\zeta$) enter the fluid equations through the dissipative part of the energy-momentum tensor,

$$T^{\rm diss}_{\mu\nu}=T_{\mu\nu}-T^{(0)}_{\mu\nu}, \tag{28}$$

where $T^{(0)}_{\mu\nu}$ is the energy-momentum tensor for the system in local equilibrium,

$$T^{(0)}_{\mu\nu}=-pg_{\mu\nu}+(p+e)u_\mu u_\nu. \tag{29}$$

The explicit form of the dissipative contribution is

$$T^{\rm diss}_{ij}=-\eta(\partial_i u_j+\partial_j u_i)-(\zeta-2/3\eta)\nabla\cdot\mathbf{u}\delta_{ij}, \tag{30}$$

where $\mathbf{u}$ is the local flow velocity. Therefore

$$T_{ij}=p\delta_{ij}+T^{\rm diss}_{ij}. \tag{31}$$

For the purpose of illustration, consider a weakly interacting system of massless scalar particles. Denote the one-particle Wigner distribution by $n_p(\mathbf{x},t)$. The integral

$$n(\mathbf{x},t)=\int\frac{d^3p}{(2\pi)^3}\,n_p(\mathbf{x},t) \tag{32}$$

gives the average number of particles at the location $\mathbf{x}$ at time $t$. The flow velocity is given by the integral

$$\mathbf{u}(\mathbf{x},t)=\frac{1}{n(\mathbf{x},t)}\int\frac{d^3p}{(2\pi)^3}\mathbf{v}_p n_p(\mathbf{x},t), \tag{33}$$

where $\mathbf{v}_p=\mathbf{p}/E_p$ is the single-particle velocity. The space-space part of the energy-momentum tensor is given by

$$T_{ij}=\int\frac{d^3p}{(2\pi)^3}p_i v_j n_p(\mathbf{x},t). \tag{34}$$

In the local rest frame, determined by $\mathbf{u}=0$, and in local thermal equilibrium, the distribution function has the form $n_p^{(0)}=1/(e^{E_p/T}\pm1)$ where the upper sign is for fermions and the lower for bosons. For small departures from equilibrium one can compute $\delta n_p=n_p-n_p^{(0)}\ll n_p^{(0)}$ from the Boltzmann equation. In the relaxation time approximation

$$\frac{\partial}{\partial t}\delta n_p+\mathbf{v}_p\cdot\nabla\delta n_p=-\delta n_p/\tau, \tag{35}$$

where $\tau$ is the collision time. Substituting the solution of the Boltzmann equation into the expression for $T_{ij}$ one eventually derives [25]

$$\eta=\frac{\tau}{15}\int\frac{d^3p}{(2\pi)^3}\frac{p^4}{E_p^2}n_p^{(0)}(1\pm n_p^{(0)}). \tag{36}$$

Thus the calculation of viscosities has been reduced to the calculation of collision times. We obtain the collision times from the cross sections with the expression

$$\tau^{-1}(p)=\int\frac{d^3p'}{(2\pi)^3}n_{p'}v_{\rm rel}\sigma(p,p'), \tag{37}$$

where $s=(p+p')^2$ and $v_{\rm rel}=s/(2EE')$. We assume that the momentum dependence is weak so that we can make the replacement $\tau^{-1}(p)=\langle\tau^{-1}(p)\rangle\equiv\tau^{-1}$. Finally, we replace the averaged product by the product of the averages, and use the fact that $\langle v_{\rm rel}\rangle=1$, to obtain

$$\tau^{-1}=n\langle\sigma(p,p')\rangle. \tag{38}$$

In a calculation of viscosities the expression that should be used for the cross section is actually the transport cross section, given by

$$\sigma=\int d(\cos\theta)\,(1-\cos\theta)\frac{d\sigma}{d(\cos\theta)}. \tag{39}$$

This can be interpreted as follows. The factor $(1-\cos\theta)$ gives a suppression of the contribution of forward scattering to the coefficient of viscosity. Physically this is a result of the fact that, when calculating viscosity, the relevant part of the dissipative energy-momentum tensor is the part that gives the energy-momentum transferred in a direction perpendicular to the forward scattering direction. The origin of this cutoff is the finite-temperature screening of the long-ranged Coulomb force [26]. This is especially important for the exchange of massless quanta. In this case, the small angle limit of the two-particle scattering cross section is dominated by the Coulomb divergence

$$\left(\frac{d\sigma}{d(\cos\theta)}\right)_{\text{Coulomb}} \sim \sin^{-4}(\theta/2). \tag{40}$$

This divergence is softened by the forward suppression factor.

These equations are modified in a straightforward way when the system contains internal degrees of freedom and/or more than one particle species. The collision time becomes

$$\tau_i^{-1} = \sum_j g_j n_j \langle \sigma_{ij} \rangle, \tag{41}$$

where the indices $i,j$ label the particle species and $g_j$ is the number of internal degrees of freedom of the $j$th species. Similarly, the expression for the viscosity generalizes to

$$\eta = \sum_i g_i \tau_i I_i\,, \tag{42}$$

where

$$I_i = \frac{1}{15}\int \frac{d^3p}{(2\pi)^3}\frac{p^4}{E_{p,i}^2} n_{p,i}^{(0)}(1 \pm n_{p,i}^{(0)}). \tag{43}$$

Next we need to calculate the two-particle scattering cross sections in the standard model. We consider the electroweak sector first and introduce the following notation. The SU(2) gauge fields are denoted $A_\mu^a$ where $\mu$ is the Lorentz index and the group index is denoted $a$. The indices $l, m, \ldots$ have values 1,2 and refer to the two components of the complex Higgs doublet. The fields are eigenstates of isospin and hypercharge (denoted $Y$). The Lagrangian is invariant under $\mathrm{SU}(2)\times \mathrm{U}(1)_Y$ transformations. It is given by

$$\mathcal{L} = \mathcal{L}_{\text{gauge field}} + \mathcal{L}_{\text{Higgs}} + \mathcal{L}_{\text{fermions}} + \mathcal{L}_{\text{Yukawa}} + \mathcal{L}_{\text{gf}}. \tag{44}$$

Each of these terms is described below.

The gauge field kinetic terms are given by

$$\mathcal{L}_{\text{gauge field}} = -\frac{1}{4}F_{\mu\nu}^a F_a^{\mu\nu} - \frac{1}{4}F_{\mu\nu}F^{\mu\nu}. \tag{45}$$

The Higgs field part of the Lagrangian is

$$\mathcal{L}_{\text{Higgs}} = (D_\mu\phi)^\dagger(D^\mu\phi) + c^2(\phi^\dagger\phi) - \lambda(\phi^\dagger\phi)^2. \tag{46}$$

The covariant derivative is

$$D_\mu = \partial_\mu + ig\frac{\tau^a}{2}A_\mu^a + ig'\frac{1}{2}B_\mu, \tag{47}$$

where the matrices $\tau^a$ are the SU(2) Pauli matrices. The complex Higgs doublet

$$\phi = \frac{1}{\sqrt{2}}\begin{pmatrix}\phi_3 + i\phi_4 \\ \phi_1 + i\phi_2\end{pmatrix} \tag{48}$$

has an electromagnetically neutral lower component and an upper component with electromagnetic charge +1. These charge assignments give an eigenstate of hypercharge.

The fermion part of the Lagrangian is given by

$$\mathcal{L}_{\text{fermions}} = \bar\psi_R i\gamma^\mu\left(\partial_\mu + i\frac{g'}{2}YB_\mu\right)\psi_R + \bar\psi_L i\gamma_\mu\left(\partial_\mu + i\frac{g'}{2}YB_\mu + i\frac{g}{2}A_\mu^a\tau_a\right)\psi_L. \tag{49}$$

There are three generations of fermions which are grouped into left-handed SU(2) doublets and right-handed SU(2) singlets. For example,

$$\psi_R = \frac{1}{2}(1+\gamma_5)e, \quad \frac{1}{2}(1+\gamma_5)u, \quad \frac{1}{2}(1+\gamma_5)d',$$

$$\psi_L = \frac{1}{2}(1-\gamma_5)\begin{pmatrix}\nu_e \\ e\end{pmatrix}, \quad \frac{1}{2}(1-\gamma_5)\begin{pmatrix}u \\ d'\end{pmatrix}_{3\text{ colors}}.$$

The primed quark states are electroweak eigenstates which are constructed as follows. We define a vector of the mass eigenstates of the charge $-1/3$ quarks: $x = (d, s, t)$. The electroweak eigenstates are denoted $x'$ and are given by $x' = Ux$ where $U$ is the unitary $3\times3$ Kobayashi-Maskawa matrix (the specific form of $U$ is not needed for this problem).

We work in the renormalizable $\mathrm{R}_\xi$ gauge where the gauge-fixing part of the Lagrangian is

$$\mathcal{L}_{\text{gf}} = -\frac{1}{2\xi}\left(\partial^\mu A_\mu^a - \frac{1}{2}\xi g v\chi^a\right)^2 - \frac{1}{2\xi}\left(\partial^\mu B_\mu - \frac{1}{2}\xi g' v\chi^2\right)^2, \tag{50}$$

and where $\chi_a = \phi_2, \phi_3, \phi_4$. We choose the Landau value of the gauge-fixing parameter $\xi \to 0$. The cross terms above combine with the cross terms from $(D_\mu\phi)^\dagger(D^\mu\phi)$ to produce total divergences which integrate to zero.

When calculating the two-body scattering cross sections, we will work to lowest order in perturbation theory, and calculate only the forward ($t$-channel) contribution since it is this term that dominates the transport cross section. We denote individual contributions to these cross sections by $\sigma_{IJ}^{(K)}$. The subscript indicates initial and final states, and the superscript indicates the field that mediates the scattering process. We represent the fermion fields by $\psi$, the SU(2) gauge boson fields by

$A$, the U(1) gauge boson fields by $B$, and the Higgs fields by $\phi$.

We need not explicitly compute all possible cross sections because many of them are not independent but can be determined by symmetries. The cross sections enclosed by square brackets can be obtained from the preceding cross sections by symmetry:

$$\sigma^A_{\psi\psi}\quad \sigma^B_{\psi\psi}\quad \left[\sigma^A_{\bar\psi\bar\psi}\quad \sigma^B_{\bar\psi\bar\psi}\quad \sigma^A_{\psi\bar\psi}\quad \sigma^B_{\psi\bar\psi}\right],$$

$$\sigma^{(A)}_{\phi\psi}\quad \sigma^{(B)}_{\phi\psi}\quad \left[\sigma^{(A)}_{\phi\bar\psi}\quad \sigma^{(B)}_{\phi\bar\psi}\quad \sigma^{(A)}_{\phi^\dagger\psi}\quad \sigma^{(B)}_{\phi^\dagger\psi}\quad \sigma^{(A)}_{\phi^\dagger\bar\psi}\quad \sigma^{(B)}_{\phi^\dagger\bar\psi}\right],$$

$$\sigma^{(A)}_{\phi\phi}\quad \sigma^{(B)}_{\phi\phi}\quad \left[\sigma^{(A)}_{\phi^\dagger\phi}\quad \sigma^{(B)}_{\phi^\dagger\phi}\quad \sigma^{(A)}_{\phi^\dagger\phi^\dagger}\quad \sigma^{(B)}_{\phi^\dagger\phi^\dagger}\right],$$

$$\sigma^{(A)}_{\phi A}\quad \left[\sigma^{(A)}_{\phi^\dagger A}\right],$$

$$\sigma^{(A)}_{\psi A}\quad \left[\sigma^{(A)}_{\bar\psi A}\right],$$

$$\sigma^{(A)}_{AA}.$$

Consider, for example, the cross section for quark-quark scattering via the exchange of an SU(2) boson:

$$\sigma^{(A)}_{\psi\psi} = \int d(\cos\theta)(1-\cos\theta)\frac{d\sigma^{(A)}_{\psi\psi}}{d(\cos\theta)}. \tag{51}$$

Using standard techniques, the $t$-channel contribution is $(-u/2t^2)C^{(A)}_{\psi\psi}$ where $C^{(A)}_{\psi\psi}$ is a constant equal to $3\pi\alpha^2/16$ with $\alpha = g^2/4\pi$. Using the Mandelstam variables $s = 4E^2$, $u = -2E^2(1+\cos\theta)$, $t = -2E^2(1-\cos\theta)$, and using the fact that the integral is dominated by the Coulomb divergence at small $\theta$, we have

$$\sigma^{(A)}_{\psi\psi} = \frac{2C^{(A)}_{\psi\psi}}{s}\int \frac{d(\cos\theta)}{(1-\cos\theta)}. \tag{52}$$

The angular integral still has a divergence at $\theta = 0$, although it has been softened by the nature of the transport cross section. A small angle cutoff is imposed on the integral: $\theta_{\min} = \alpha^{3/2}$. The origin of this cutoff is that the long-ranged Coulomb force gets Debye-screened at finite temperature. This screening physics has been discussed in the field theory context in [25]. Finally, we use $\langle 1/s\rangle = (1/2)\langle 1/E\rangle^2$, $\langle 1/E\rangle = 1/(2.2T)$, and $n = 3T^2\zeta(3)/(4\pi^2)$ (where $\zeta$ is the Riemann $\zeta$ function) for fermions. This gives

$$\tau^{-1} = \frac{3T^2\zeta(3)}{4\pi^2}\left(\frac{1}{2.2T}\right)^2\frac{9\pi\alpha^2}{16}\ln(1/\alpha). \tag{53}$$

Note that, at the very least, the absolute magnitude of the argument of the logarithm cannot be precisely determined using this simple calculational approach.

In general the $t$-channel contribution to each cross section has the same form,

$$\frac{d\sigma^{(K)}_{IJ}}{d(\cos\theta)} = -C^{(K)}_{IJ}\frac{u}{2t^2}. \tag{54}$$

We obtain the following expressions for the coefficients:

$$\begin{aligned}
C^A_{\phi\phi} &= 3\pi\alpha^2/4,\\
C^{(B)}_{\phi\phi} &= \pi(\alpha')^2/4,\\
C^{(A)}_{\psi\psi} &= 3\pi\alpha^2/16,\\
C^{(B)}_{\psi\psi} &= Y^2Y^2\pi(\alpha')^2/16,\\
C^{(A)}_{\psi\phi} &= 3\pi\alpha^2/8,\\
C^{(B)}_{\psi\phi} &= Y^2\pi(\alpha')^2/8,\\
C^{(A)}_{\phi A} &= 2\pi\alpha^2,\\
C^{(A)}_{\psi A} &= \pi\alpha^2,\\
C^{(A)}_{AA} &= 16\pi\alpha^2/3,
\end{aligned} \tag{55}$$

where $\alpha = g^2/4\pi$, $\alpha' = g'^2/4\pi$, and $g = 0.637$, $g' = 0.344$. Note that the cross sections that are mediated by the U(1) gauge boson and have a fermion in the final state depend on the square of the fermion hypercharge. For notational convenience we make the definitions $C^{(B)}_{\psi\psi} = Y^2Y^2\tilde C^{(B)}_{\psi\psi}$ and $C^{(B)}_{\psi\phi} = Y^2\tilde C^{(B)}_{\psi\phi}$.

Several comments about the numerical factors involved in these expressions are in order. We work in the high-temperature symmetric phase and in the limit of small Higgs coupling. In this limit, all of the fields are massless. In particular, the fermion fields are massless and so there are only two independent Dirac spinors. Therefore, we work with a Lagrangian that contains only left-handed fermions and use the usual normalization factors for massless spinors.

Note that when the scattering process involves identical particles the contribution from the $u$ channel is nonzero and equal to the $t$-channel contribution. In the limit $\theta \to \pi$ the $u$ channel gives the backward scattering peak in the two-particle cross section. When calculating viscosity, the $u$ channel contributes to the transport cross section a term of the form

$$\sigma = \int d(\cos\theta)(1+\cos\theta)\frac{d\sigma}{d(\cos\theta)}. \tag{56}$$

The factor $(1+\cos\theta)$ gives a suppression of the contribution of the backward scattering divergence to the viscosity. As was discussed earlier, this factor is a result of the fact that viscosity involves the transfer of energy-momentum perpendicular to the scattering direction. For identical particles, therefore, the $t$-channel result should be multiplied by a factor of 2. Also, the terms which have antiparticles on external lines (indicated in the square brackets earlier) can be included by multiplying the above expressions by the appropriate numerical

factors.

Finally, we note that there should be an extra factor of 2 in the expressions for $d\sigma/d(\cos\theta)$ when the scattering involves identical particles because scattering through angles of $\theta$ and $\pi-\theta$ is indistinguishable. Similarly, however, in the expression for the collision time there should be a factor of 1/2 when the cross section involves identical particles, to avoid double counting. These two factors cancel each other and we omit them both in our intermediate results for notational simplicity.

These results for the cross sections allow us to obtain expressions for the collision times. We use the following results. For fermions, the number density is given by $n \equiv n_F = 3T^3\zeta(3)/(4\pi)$, and $\langle 1/E\rangle = 1/(2.2T)$; for bosons, $n \equiv n_B = T^3\zeta(3)/\pi$ and $\langle 1/E\rangle = 1/(1.5T)$. The number of internal degrees of freedom are obtained as follows. For each generation, there is one lepton doublet and one quark doublet which carries three colors, and each fermion has two spin states. This gives $g_\psi = (2 + 3\times 2)\times 3\times 2 = 48$ for three generations. There are $(N^2-1)$ SU(N) gauge bosons, each of which has two spin states, which gives $g_A = 2\times 3 = 6$. The two isospin states of the Higgs doublet give $g_\phi = 2$. Finally, we use $\sum_\psi Y^2 = 8/3$.

The expressions for the inverse collision times take the forms

$$\tau_A^{-1} = \frac{3\ln(1/\alpha)}{1.5T}\left(\frac{n_B}{1.5T}2g_\phi C_{\phi A}^{(A)} + \frac{n_B}{1.5T}2g_A C_{AA}^{(A)} + \frac{n_F}{2.2T}2g_\psi C_{A\psi}^{(A)}\right), \tag{57}$$

$$\tau_\phi^{-1} = \frac{3\ln(1/\alpha)}{1.5T}\left(\frac{n_B}{1.5T}3g_\phi C_{\phi\phi}^{(A)} + \frac{n_B}{1.5T}g_A C_{A\phi}^{(A)} + \frac{n_F}{2.2T}2g_\psi C_{\psi\phi}^{(A)}\right) + \frac{3\ln(1/\alpha')}{1.5T}\left(\frac{n_B}{1.5T}3g_\phi C_{\phi\phi}^{(B)} + \frac{n_F}{2.2T}2\times 2\times 8/3\tilde{C}_{\psi\phi}^{(B)}\right), \tag{58}$$

$$\tau_\psi^{-1} = \frac{3\ln(1/\alpha)}{2.2T}\left(\frac{n_B}{1.5T}2g_\phi C_{\phi\psi}^{(A)} + \frac{n_B}{1.5T}g_A C_{A\psi}^{(A)} + \frac{n_F}{2.2T}(2g_\psi + 2N_c)C_{\psi\psi}^{(A)}\right) + \frac{3\ln(1/\alpha')}{2.2T}\left[\frac{n_B}{1.5T}2g_\phi C_{\phi\psi}^{(B)} + \frac{n_F}{2.2T}\left(\frac{32}{3}Y^2 + 2N_cY^4\right)\tilde{C}_{\psi\psi}^{(B)}\right]. \tag{59}$$

In the last expression, $N_c$ is the number of colors if the fermion is a quark and one if the fermion is a lepton. It is straightforward to include the contributions of the strong interactions. Using the notation defined in Eq. (54) where $q$ and $g$ indicate quark and gluon degrees of freedom, respectively, the coefficients for the $t$-channel contributions to the quark and gluon scattering matrix elements are [27]

$$C_{gg} = 9\pi\alpha_s^2/2,$$
$$C_{qq} = C_{q\bar{q}} = C_{\bar{q}\bar{q}} = 8\pi\alpha_s^2/9, \tag{60}$$
$$C_{qg} = C_{\bar{q}g} = 2\pi\alpha_s^2.$$

We consider $N_F$=6 flavors and thus the number of quark degrees of freedom is $g_q$ = 2(spin) × 3(color) × 6(flavor) = 36. The number of gluon degrees of freedom is $g_g$ = 2(spin) × $(N_c^2-1)$ = 16, with $N_c$ = 3. The inverse collision times for gluons, and for quarks due to gluon interactions, are given by

$$\tau_g^{-1} = \frac{3\ln(1/\alpha_s)}{1.5T}\left(\frac{n_B}{1.5T}2g_g C_{gg} + \frac{n_F}{2.2T}2g_q C_{qg}\right), \tag{61}$$

$$(\tau_q^{(g)})^{-1} = \frac{3\ln(1/\alpha_s)}{2.2T}\left(\frac{n_B}{1.5T}g_g C_{qg} + \frac{n_F}{2.2T}6(2N_F+1)C_{qq}\right). \tag{62}$$

We define inverse collision times for leptons and quarks, $\tau_l^{-1} = \tau_\psi^{-1}$ and $\tau_q^{-1} = \tau_\psi^{-1} + (\tau_q^{(g)})^{-1}$.

The viscosities are obtained from Eqs. (42) and (43). Defining

$$I_F = \int dx \frac{x^4}{1+e^x}\left(1 - \frac{1}{1+e^x}\right) = \frac{7\pi^4}{30},$$
$$I_B = \int dx \frac{x^4}{e^x-1}\left(1 - \frac{1}{e^x-1}\right) = \frac{4\pi^4}{15},$$

we have

$$\eta = \frac{T^4}{30\pi^2}\left[2\left(\sum_l \tau_l + \sum_q \tau_q\right)I_F + (2g_\phi\tau_\phi + g_A\tau_A + g_g\tau_g)I_B\right]. \tag{63}$$

We use the standard values for the electroweak couplings, $\alpha$ and $\alpha'$. For the strong coupling we estimate [28]

$$\alpha_s = \frac{6\pi}{(11N_c - 2N_F)\ln(10.6\,T/T_{\rm QCD})}, \tag{64}$$

where $T_{\rm QCD}$ = 150 MeV, and evaluate at $T$ = 97.27 GeV. This gives $\alpha_s$ = 0.102. The final result is $\eta = 82.5\,T^3$.

## VI. EVOLUTION OF THE UNIVERSE

In this section we study the evolution of the Universe as it passes through the electroweak phase transition. This must be done numerically because the evolution is de-

scribed by coupled integral and differential equations.

To get a first impression as to how much the Universe must supercool before nucleation begins, we plot the nucleation time in Fig. 1 as a function of temperature. Nucleation time is defined by

$$\tau_{\text{nucleation}} = \frac{4\pi r_*^3}{3} I \ . \tag{65}$$

This is the characteristic time scale to make the transition in the absence of bubble growth; that is, the transition would complete only because every point in space had been nucleated. The solid curve represents our best estimate of the nucleation rate, as discussed in previous sections. The dashed curve shows what happens when the finite-size correction to the critical bubbles is neglected; see Eq. (23). Although this curve is labeled *sharp surface*, this is not an entirely correct designation. The reason is that it does make use of the surface tension $\sigma$, and this quantity is computed with a smooth surface of finite thickness, albeit planar. The dot-dashed curve shows what happens when the preexponential factor in the rate is taken to be $T_c^4$ rather than the expression given by Eq. (5). Both approximations differ from the best estimate of the nucleation time by many orders of magnitude. On the other hand, one may say that use of the more sophisticated estimates for the bubble free energy and the preexponential factor simply results in a delay of the onset of the phase transition.

To relate the expansion scale of the Universe to the local time we recall Eq. (11). Defining $\Delta t = t - t_c$ and $\Delta R = R - 1$, and using the equation of state from Sec. III, we obtain

$$\Delta t = 4.97 \times 10^{-11} \, \Delta R \text{ sec.} \tag{66}$$

Comparison with Fig. 1 suggests that we will see supercooling of about 0.25% in the temperature.

Figure 2 shows the temperature as a function of the scale factor. The solid curve represents the Maxwell construction for phase coexistence at $T_c$ and generates no entropy. The dashed curve is a result of solving numerically the coupled equations discussed earlier in the paper. The difference between these two curves is remarkable. Nucleation does not even begin until long after an idealized adiabatic Maxwell phase transition would have completed. However, once nucleation begins, the transition proceeds and completes in a much shorter time interval. For practical purposes, nucleation begins at the bottom of the cooling line. Thereafter, nucleation and growth of bubbles release latent heat, which causes the temperature to rise. Once the transition is completed, the Universe again cools. A very small amount of entropy is generated during the transition because the Universe is out of equilibrium. The amount generated can be inferred by comparing $T^3$ for the dashed curve to $T^3$ for the solid curve. An earlier treatment of the electroweak phase transition gave a trajectory of temperature vs time very similar in shape to this one; see Fig. 10(a) of Ref. [13].

Figure 3 shows the fraction of space which has been converted from the high-temperature symmetric $S$ phase to the low-temperature asymmetric $A$ phase as a function of scale factor. The solid curve is the Maxwell idealiza-

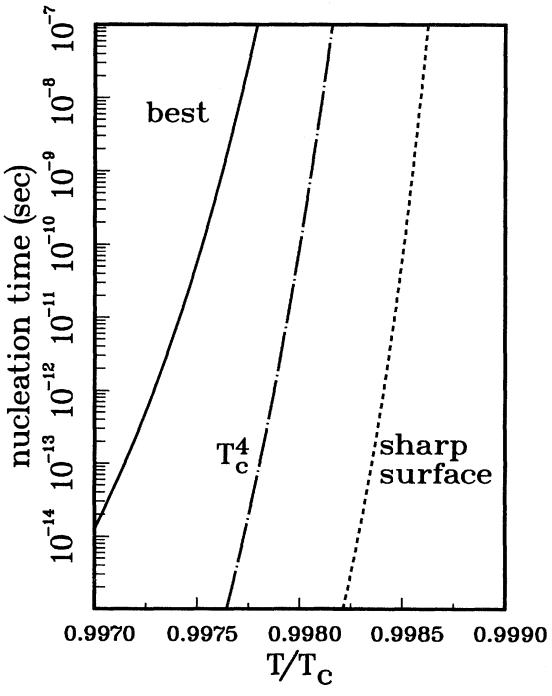


FIG. 1. The nucleation time, as defined in the text, as a function of temperature. The solid curve represents our best estimate. The dashed curve approximates the bubble free energy as a sum of volume plus surface terms, and neglects the finite-size correction. The dot-dashed curve approximates the preexponential factor in the rate by $T_c^4$.

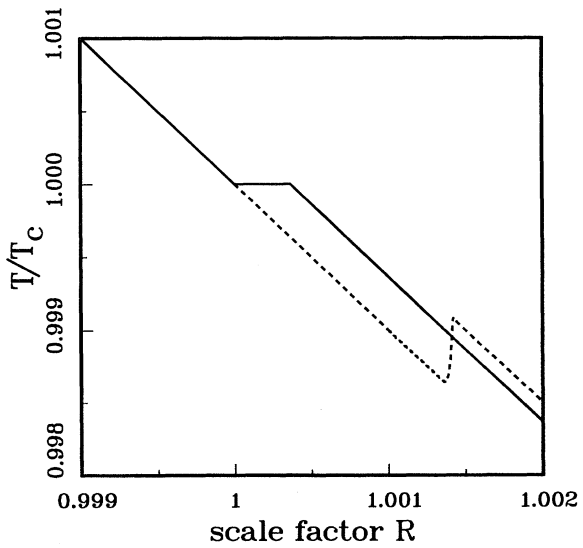


FIG. 2. Temperature vs scale factor. The solid curve represents the adiabatic Maxwell construction for phase coexistence at $T_c$. The dashed curve represents the results of numerically integrating the dynamical equations of motion.

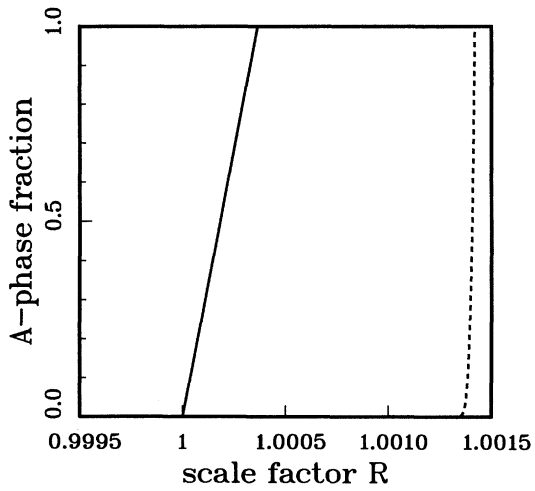


FIG. 3. The $A$-phase fraction $f$ vs scale factor. The solid curve represents the adiabatic Maxwell construction for phase coexistence at $T_c$. The dashed curve represents the results of numerically integrating the dynamical equations of motion.

tion and the dashed curve is the result of our dynamical equations. It is another way of showing that the finite transition rate delays the onset of the transition, but once it begins it completes in a very short time.

Figure 4 shows the average bubble density

$$n(t) = \int_{t_c}^{t} dt' I(T(t'))[1 - f(t')] \tag{67}$$

as a function of time. Bubble nucleation is not noticeable until about $6.5 \times 10^{-14}$ sec after the Universe has cooled to $T_c$. At about $6.87 \times 10^{-14}$ sec, bubble nucleation has already turned off because of reheating to higher temperatures. The transition is not completed until about $7.05 \times 10^{-14}$ sec, as indicated by the termination point on the curve.

Figure 5 shows the fraction of space $f(t)$ which has made the conversion to the $A$ phase. One could say, from the point of view of this quantity, that the transition requires only about $3 \times 10^{-15}$ sec from start to completion. This is much shorter than the characteristic expansion time scale of the Universe, which is $dt/dR = 5 \times 10^{-11}$ sec.

Figure 6 shows the average bubble radius, defined by

$$\frac{4\pi \bar{r}_*^3}{3} = \frac{f}{n}, \tag{68}$$

as a function of the $A$-phase fraction $f$. When nucleation first turns on, the radius of a critical-size bubble is very small. As the transition proceeds, the average radius increases. At first it is because reheating brings the Universe closer to the critical temperature; as the temperature goes up, so does the size of newly nucleated bubbles. Eventually nucleation turns off, and bubbles increase in size only because of growth.

Figure 7 shows the average bubble radius as a function of time. There is a linear relation between the average radius and time, indicating constant radial growth velocity, after about $6.87 \times 10^{-14}$ sec. This is the time when nucleation has just turned off. At this time only about 10% of the Universe has been converted to the new phase. The remaining 90% is converted because of bubble growth. From the figure it may be seen that this growth velocity is about 0.82 times the speed of light.

A useful quantity for baryogenesis is the value of the Higgs condensate inside the bubble. For the actual range of temperatures seen here during the transition, we know that $\phi_A/T_c \approx 0.54 - 0.58$. At zero temperature the condensate has the known value $\phi_A = 246$ GeV $= 2.53\ T_c$.

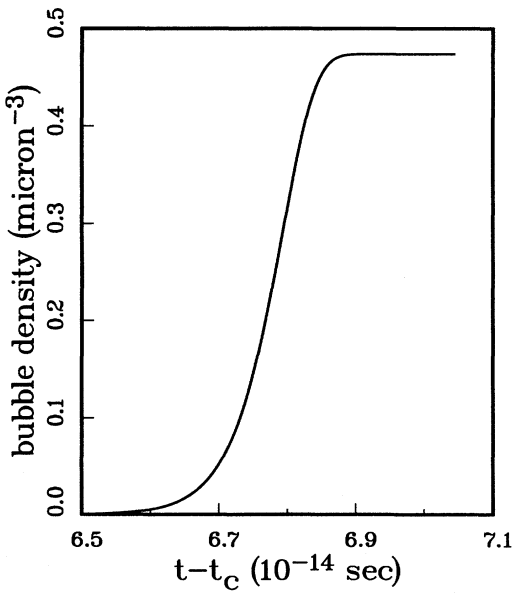


FIG. 4. The density of $A$-phase bubbles as a function of time.

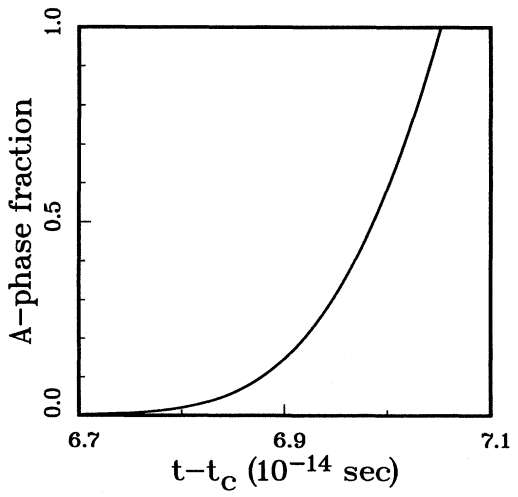


FIG. 5. The fraction of space which has been converted to the $A$ phase as a function of time.

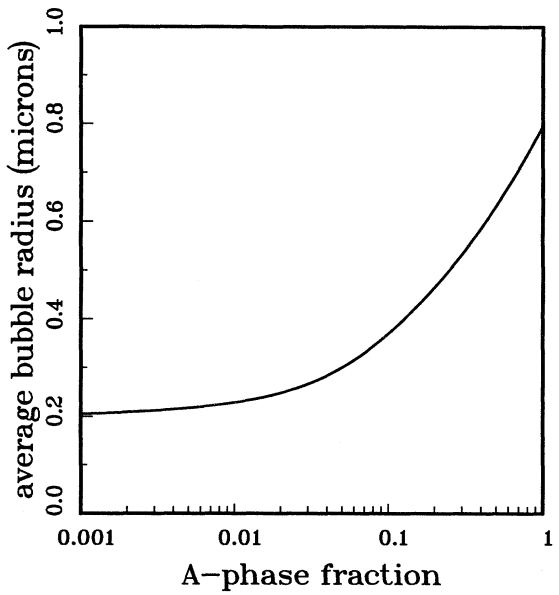


FIG. 6. The average bubble radius as a function of the $A$-phase fraction.

A larger value than that seen during the transition would have been more favorable for baryogenesis. However, this is intimately tied to the very small latent heat in the standard model. Extended models of the electroweak interactions could have larger latent heats and larger values of the Higgs condensate inside the bubbles.

We must add a cautionary note. When the fraction of space occupied by bubbles exceeds about 50%, interactions among the bubbles probably cannot be neglected. It is unlikely, though, that further improvements in the dynamics would qualitatively change the current picture of the transition. Indeed, crude estimates of the effects of bubble fusion on the dynamics of the QCD transition indicate that the transition completes only a little faster, and that the average bubble size is greater [20]. Further developments on this topic would be welcome.

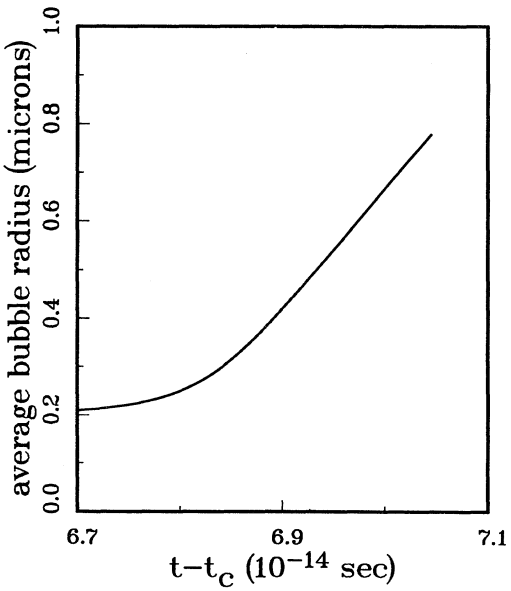


FIG. 7. The average bubble radius as a function of time.

## VII. CONCLUSIONS

We have analyzed in detail the dynamics of the electroweak phase transition during the early Universe. We used the ring-improved effective potential for the standard model. From this potential we extracted the equation of state, the surface free energy, and the correlation lengths. We calculated the viscosity in the high-temperature $S$ phase, which is an important factor in the nucleation rate, and which may be useful in other contexts as well. We used a recently computed expression for the preexponential factor in the nucleation rate, and took into account the finite-size effect for critical bubbles. We used a recent expression for the growth velocity of bubbles. All of these ingredients were joined together with a rate equation which allows for completion of the phase transition. Coupling this rate equation with Einstein's equations allowed us to solve for the dynamical evolution of the Universe through the electroweak phase transition.

We computed the temperature, fraction of space converted, bubble density, and average bubble radius as functions of time. The temporal evolution of the Universe does not resemble an adiabatic Maxwell construction of coexisting phases. This is remarkable because the characteristic expansion time scale of the Universe is $10^{-11}$ sec, very short compared to the characteristic time scale $10^{-26}$ sec of electroweak theory. The explanation is that the electroweak phase transition, at least as studied here, is first order but very weak. The pressure difference between the two phases near $T_c$ is very small. This leads to times and structures which are mesoscopic during the phase transition.

The Universe is out of equilibrium during the phase transition. This is one of the necessary ingredients for baryogenesis. Baryon number changing processes are expected to take place in the bubble surface; therefore, our results should be useful for such studies. They can also be easily repeated for extensions of the standard model.

Improvements to many aspects of our study may be considered, especially for the late stage of the phase transition when bubbles begin to overlap. However, it is becoming clear that a quantitative analysis of the electroweak phase transition during the early Universe can be put on firm footing, and this will help us to contemplate our origins via baryogenesis.

## ACKNOWLEDGMENTS

We are grateful to K. Kajantie, P. Lichard, L. McLerran, M. Prakash, and M. Shaposhnikov for discussions. This work was supported by the Minnesota Supercomputer Institute and by the U.S. Department of Energy under Grant No. DOE/DE-FG02-87ER40328.

[1] D. A. Kirzhnits and A. D. Linde, Phys. Lett. **42B**, 471 (1972); L. Dolan and R. Jackiw, Phys. Rev. D **9**, 3320 (1974); S. Weinberg, *ibid.* **9**, 3357 (1974).
[2] G. 't Hooft, Phys. Rev. Lett. **37**, 8 (1976); Phys. Rev. D **14**, 3432 (1976); A. D. Linde, Phys. Lett. **70B**, 306 (1977); S. Dimopoulos and L. Susskind, Phys. Rev. D **18**, 4500 (1978); N. S. Manton, *ibid.* **28**, 2019 (1984); F. Klinkhamer and N. S. Manton, *ibid.* **30**, 2212 (1984); V. A. Kuzmin, V. A. Rubakov, and M. E. Shaposhnikov, Phys. Lett. **155B**, 36 (1985); P. Arnold and L. McLerran, Phys. Rev. D **36**, 581 (1987); **37**, 1020 (1988); L. Carson, Xu Li, L. McLerran, and R. T. Wang, *ibid.* **42**, 2127 (1990).
[3] M. E. Shaposhnikov, Pis'ma Zh. Eksp. Teor. Fiz. **44**, 364 (1986) [JETP Lett. **44**, 465 (1986)]; Nucl. Phys. **B287**, 757 (1987); **B299**, 797 (1988); L. McLerran, Phys. Rev. Lett. **62**, 1075 (1989); A. I. Bochkarev, S. Yu. Khlebnikov, and M. E. Shaposhnikov, Nucl. Phys. **B329**, 493 (1990); A. D. Cohen, D. B. Kaplan, and A. E. Nelson, Phys. Lett. B **246**, 561 (1990); **349**, 727 (1991).
[4] N. Turok and J. Zadrozny, Phys. Rev. Lett. **65**, 2331 (1990); Nucl. Phys. **B358**, 471 (1991); L. McLerran, M. Shaposhnikov, N. Turok, and M. Voloshin, Phys. Lett. B **256**, 561 (1991).
[5] M. E. Carrington, Phys. Rev. D **45**, 2933 (1992).
[6] A. D. Linde, Nucl. Phys. **B216**, 421 (1983).
[7] K. Enqvist, J. Ignatius, K. Kajantie, and K. Rummukainen, Phys. Rev. D **45**, 3415 (1992).
[8] N. Turok, Phys. Rev. Lett. **68**, 1803 (1992).
[9] M. Dine, R. G. Leigh, P. Huet, A. D. Linde, and D. Linde, Phys. Rev. D **46**, 550 (1992).
[10] B. H. Liu, L. McLerran, and N. Turok, Phys. Rev. D **46**, 2668 (1992).
[11] L. P. Csernai and J. I. Kapusta, Phys. Rev. D **46**, 1379 (1992).
[12] L. P. Csernai and J. I. Kapusta, Phys. Rev. Lett. **69**, 737 (1992).
[13] K. Enqvist, J. Ignatius, K. Kajantie, and K. Rummukainen, Phys. Rev. D **45**, 3415 (1992).
[14] R. Becker and W. Döring, Ann. Phys. (N.Y.) **24**, 719 (1935).
[15] J. S. Langer, Ann. Phys. (N.Y.) **54**, 258 (1969).
[16] K. Kawasaki, J. Stat. Phys. **12**, 365 (1975).
[17] L. A. Turski and J. S. Langer, Phys. Rev. A **22**, 2189 (1980).
[18] J. S. Langer and A. J. Schwartz, Phys. Rev. A **21**, 948 (1980).
[19] A. H. Guth and E. J. Weinberg, Phys. Rev. D **23**, 876 (1981).
[20] L. P. Csernai, J. I. Kapusta, Gy. Kluge, and E. E. Zabrodin, Z. Phys. C (to be published).
[21] A. L. Fetter and J. D. Walecka, *Quantum Theory of Many-Particle Systems* (McGraw-Hill, New York, 1971).
[22] J. I. Kapusta, *Finite Temperature Field Theory* (Cambridge University Press, Cambridge, England, 1989).
[23] J. W. Cahn and J. E. Hilliard, J. Chem. Phys. **28**, 258 (1958); **31**, 688 (1959).
[24] A. H. Falls, L. E. Scriven, and H. T. Davis, J. Chem. Phys. **75**, 3986 (1981).
[25] A. Hosoya and K. Kajantie, Nucl. Phys. **B250**, 666 (1985).
[26] F. Reif, *Fundamentals of Statistical and Thermal Physics* (McGraw-Hill, New York, 1965).
[27] B. L. Combridge, J. Kripfganz, and J. Ranft, Phys. Lett. **70B**, 234 (1977).
[28] J. I. Kapusta, Phys. Rev. D **46**, 4749 (1992).